Contents lists available at [SciVerse ScienceDirect](http://www.elsevier.com/locate/gsf)

China University of Geosciences (Beijing)

Geoscience Frontiers

journal homepage: [www.elsevier.com/locate/gsf](http://www.elsevier.com/locate/gsf)

Research paper

## Structure of the Panzhihua intrusion and its Fe-Ti-V deposit, China

Arnaud Pêcher<sup>a,\*</sup>, Nicholas Arndt<sup>a</sup>, Alexander Jean<sup>a</sup>, Arthur Bauville<sup>a</sup>, Clement Ganino<sup>a,b</sup>, Charlotte Athurion<sup>a</sup><sup>a</sup> *ISTerre, Université Joseph Fourier de Grenoble, CNRS, 1381 rue de la Piscine, 38400 Saint Martin d'Hères, France*<sup>b</sup> *Geoazur, Université de Nice-Sophia Antipolis, CNRS/IRD, Parc Valrose, 06108 Nice, France*

## ARTICLE INFO

## Article history:

Received 19 September 2012

Received in revised form

4 February 2013

Accepted 7 February 2013

Available online 27 February 2013

## Keywords:

Fe-Ti-V deposit

Intrusion

Structure

Skarn

Tectonics

## ABSTRACT

The Panzhihua intrusion in southwest China is part of the Emeishan large igneous province and host of a large Fe-Ti-V ore deposit. In previous interpretations it was considered to be a layered, differentiated sill with the ore deposits at its base. New structural and petrological data suggest instead that the intrusion has an open S-shape, with two near-concordant segments joined by a discordant dyke-like segment. During emplacement of the main intrusion, multiple generations of mafic dykes invaded carbonate wall rocks, producing a large contact aureole. In the central segment, magmatic layering is oriented oblique to the walls of the intrusion. This layering cannot have formed by crystal settling or in-situ growth on the floor of the intrusion; instead we propose that it resulted from inward solidification of multiple, individually operating, convection cells. Ore formation was triggered by interaction of magma with carbonate wall rocks.

© 2013, China University of Geosciences (Beijing) and Peking University. Production and hosting by Elsevier B.V. All rights reserved.

## 1. Introduction and geological setting

The Emeishan large igneous province, emplaced 260 Ma ago in SW China, contains several large mafic-ultramafic ore bearing intrusions (Zhang et al., 2009; Shellnutt et al., 2011), such as Hongge intrusion (Zhong et al., 2002, 2003), Xinjie intrusion (Zhong et al., 2004, 2011), Baima (Wang and Zhou, 2006) or Panzhihua. In this paper we discuss the structure of the large Fe-Ti-V-bearing Panzhihua intrusion, and its implications for the formation of the ore deposit. The geological setting of the intrusion and its ore deposits has been discussed in many other papers (Zhou et al., 2002, 2005, 2008; Ganino et al., 2008; Pang et al., 2008) and will only be briefly outlined here.

The intrusion had previously been interpreted as a sill-like body that dips 50–60°NW and extends NE–SW for about 19 km (Fig. 1).

It is layered throughout (Fig. 2), being characterized by decimetre-to centimetre-scale layers of contrasting mineralogy and grain size. Zhou et al. (2005) and Pang et al. (2008) reported that the intrusion is differentiated from highly mafic, often magnetite-rich, melano-gabbro at the base, grading through normal gabbro to leucogabbro near the top. It intrudes late Proterozoic dolostones, marls and quartzites, which, at the contact of the intrusion, have been transformed into marbles and skarns within an up to 300-m-thick contact aureole. The upper aureole is not observed because the NW margin of the intrusion is cut by a fault and intruded by syenite.

The intrusion hosts several large magmatic Fe-Ti-V oxide ore deposits. These occur as magnetite-rich cumulate layers or discordant lenses that are distributed along the southeast margin of the intrusion, in some cases extending down into the wall rock marble (Zhou et al., 2005).

## 2. Methods

During field trips in February–March 2010 and November 2011, we remapped the northern part of the intrusion and part of its contact aureole, and conducted a systematic structural investigation, focussing mainly on the intrusion itself. The large open-pit mines of Lanjian and Zujiabaobao provide excellent exposure (Fig. 2a) which is largely absent in the surrounding countryside. We paid particular attention to the contact between the gabbro and

\* Corresponding author. Tel.: +33 476 635 908; fax: +33 476 635 252.

E-mail address: [arnaud.pecher@ujf-grenoble.fr](mailto:arnaud.pecher@ujf-grenoble.fr) (A. Pêcher).

Peer-review under responsibility of China University of Geosciences (Beijing)



Production and hosting by Elsevier

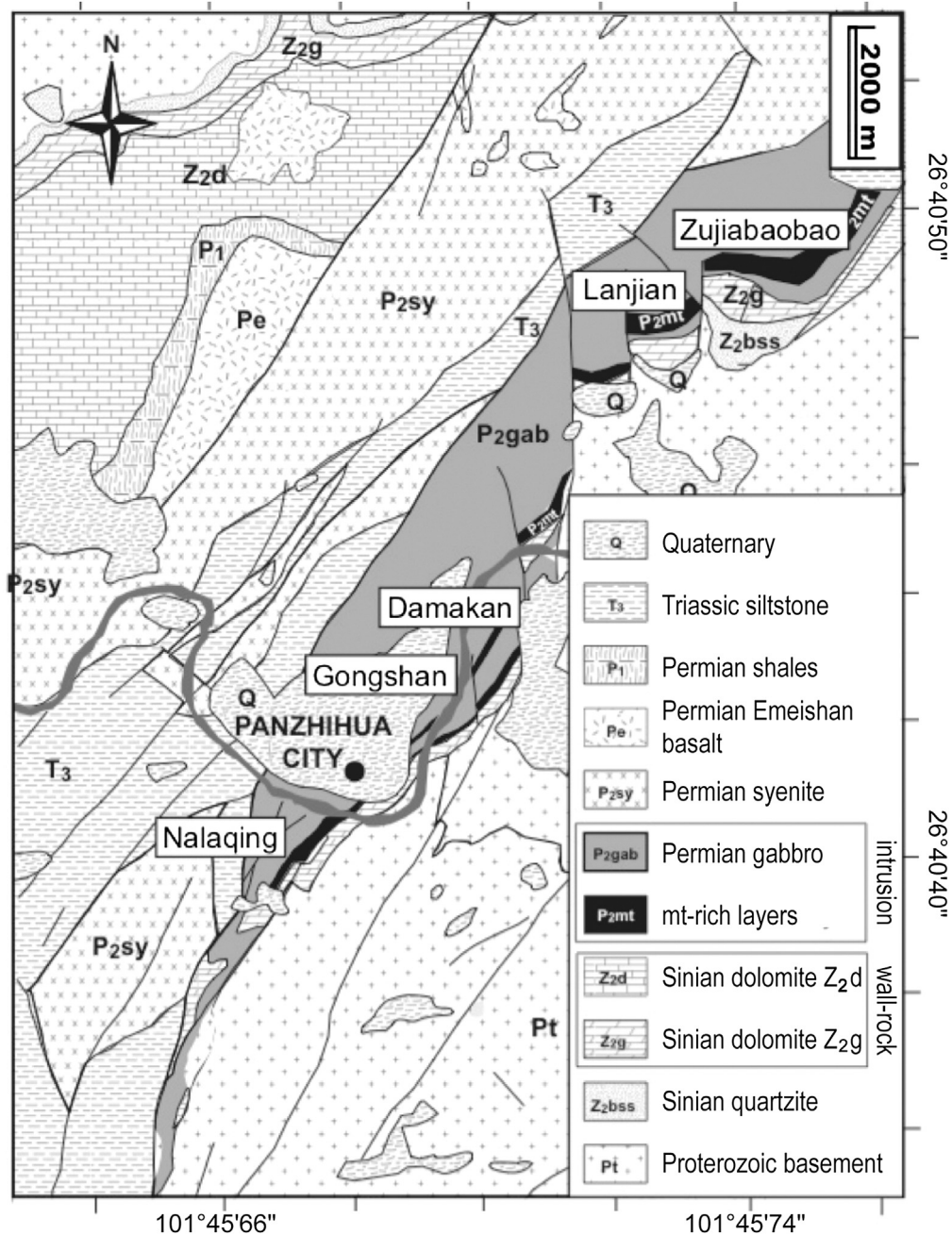


Figure 1. Geological map of the Panzhihua intrusion (Zhou et al., 2005).

rocks of the contact aureole along the SE margin of the intrusion, on the types and structure of mafic dykes in the aureole, and on orientation of layering and foliation in both the intrusion and country rock, relative to that of the exposed contact. We also made additional structural measurements and took samples in small quarries in the southern part of the intrusion to the west of Panzhihua city (Nalaqing, Fig. 1) and in several outcrops of unmetamorphosed dolomites and other sedimentary rocks to the east and north.

The layering in the intrusion is conspicuous in the walls of the open-pit mines (Fig. 2), particularly when rain washes away the dust. Its direct measurement by compass requires care because of the presence of zones rich in magnetite. We systematically avoided areas where magnetite was visible, and we repeatedly checked

compass directions using GPS reference points. Nonetheless, we cannot exclude the possibility that a few measurements are influenced by undetected concentrations of magnetite. Our maps and stereograms are based on ca. 130 measurements of banding in the gabbro, and ca. 50 measurements of foliation and/or layering in the rocks of the contact aureole. Most measurements were made in the Lanjian and Zujiabaobao open pits.

We studied thin sections to establish the metamorphic mineral assemblages in rocks of the aureole and conducted some in-situ analyses using X-ray microfluorescence, a scanning electron microscope and an electron microprobe at the Institut de Sciences de la Terre (ISTerre) in Grenoble. Major and trace element compositions of magmatic, metasedimentary and sedimentary rocks are reported by Ganino et al. (2013a).

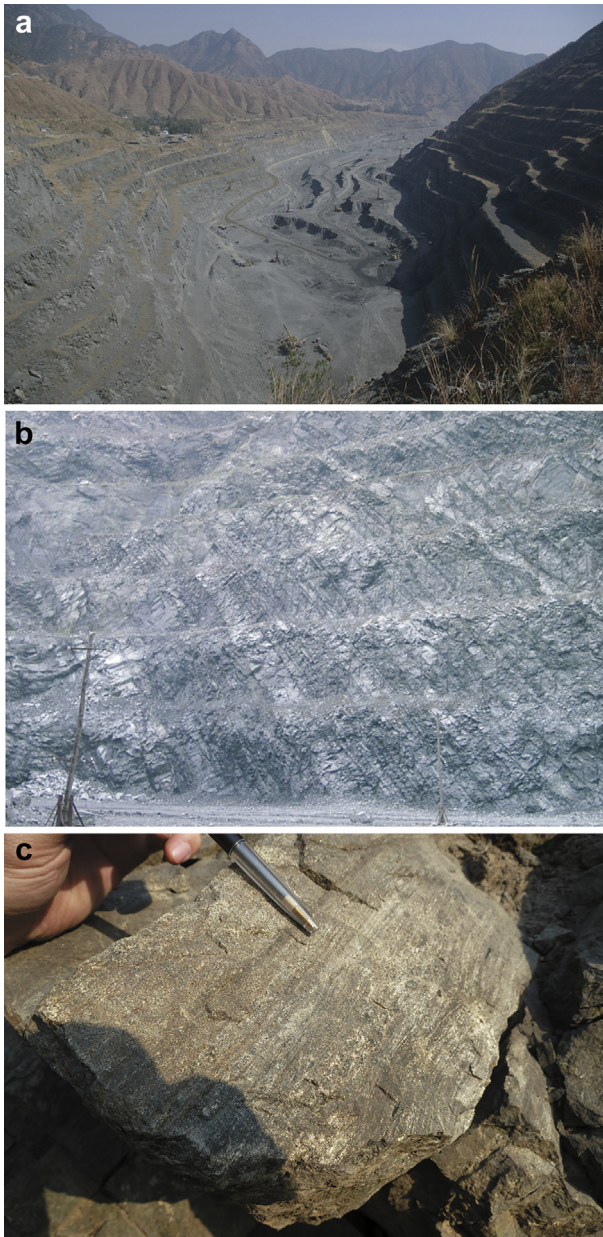


**Figure 2.** (a) Photographs of the Lanjian (in the foreground) and Zujiabaobao (back) open pits; (b) Magmatic layering in the wall of the Lanjian open pit; (c) Magmatic layering, outcrop scale.

### 3. Results

#### 3.1. Global structure of the intrusion

The main fabric of the intrusion is the centimetre- to metre-scale, textural and mineralogical banding or layering (Fig. 2c). This layering is due to changes in the relative proportions of dark and light-coloured minerals (clinopyroxene, olivine and magnetite as opposed to plagioclase feldspar) and variations in grain size. The layering is locally highlighted by the injection, parallel or slightly oblique to the layering, of light-coloured veins of leucogabbro (Fig. 2b). A clear preferred orientation of mineral grains is irregularly developed, particularly in the light-coloured bands. In places this foliation is oblique to the banding but in general it is parallel and there is no evidence that the banding is also a plane of flattening.

The western original intrusive contact of the intrusion remains unknown, due to a major SSE–NNW fault, which brings unmetamorphosed Triassic pelites and sandstones against the Permian gabbro (Fig. 3). The possible offset of the western part of the gabbro due to this fault remains unknown, as does the nature of NNW part of the intrusion. To the south of Panzhuhua city, the original intrusive contact of the gabbro is partly obliterated by nearly coeval granites and syenites, but farther north, in Lanjian area, the intrusion invaded a series of Proterozoic dolomites with minor intercalated quartzites and shales. In this area, a strong contact metamorphic imprint is observed (see Section 3.3). Considering the orientations of (a) the eastern contact, (b) the internal contacts inside the intrusion, i.e. the contact between leucogabbro and melanogabbro and (c) the ore lenses, we can distinguish three segments of the intrusion (Fig. 3).

- (i) A *southern segment* (Nalaqing to Gongshan between latitudes N 26°33' and 26°35'), where the intrusion is oriented at ca. 045°. We do not know the regional dip of the eastern gabbro contact in this area and cannot calculate the obliquity between the layering and footwall of the intrusion. But the apparent skew between the fabric in the gabbro (best plane: 050°/70°N for Zone A, 062°/40° for the Zone B, Fig. 3) and both the leucogabbro-melanogabbro contact and the footwall contact is low.
- (ii) A *central segment*, between latitudes N 26°35' and 26°38', where the overall trend of the intrusion is about 015°, and where there is a strong obliquity between the layering trace and the intrusion orientation. According to the published map (Zhou et al., 2005), to the south of 26°36.5', the cartographic orientation of the intrusive contact is related to an NS fault, which forms the eastern wall of the intrusion. However, we found no trace of this fault in the intrusion itself and believe that this fault, if it exists, has only a small displacement. We emphasize that, throughout this section, the internal contact between melanogabbro and leucogabbro is oriented at 015°; i.e., at the same general direction as the eastern contact of the intrusion. North of 26°36.5', in Lanjian area, the intrusive contact of the gabbro is disrupted in places by minor N–S trending faults and turns SW–NE. In the parts of the Lanjian and Zujiabaobao open pits that we studied in most detail (Figs. 4 and 5, and Section 3.2), the gabbro-marble contact is oriented at ca. 040°E/45°NW. In the same area, the layering in the intrusion (calculated using the best plans from measurements in areas C to F, Fig. 3) is ca. 110°E/50°N. The layering is therefore at a distinct angle to the contact, with an obliquity of about 40°.
- (iii) A *northern segment* (Zujiabaobao pit), where the intrusion is oriented N110°E. In this part of the segment, the orientation (strike) of the banding differs little from that observed in the central segment (best plane, area G: N109°E/45°N, Fig. 3), and, as in the southern segment, it is parallel to strike of the contact. Here we could not estimate the actual obliquity between the layering and the footwall. In the north-eastern part of Zujiabaobao pit, the orientation of the layering and the orientation of the contact change slightly to about 065°E. A few remnants of dolomites pinched below the Triassic sandstones indicate that, in this last segment, the gabbro layering is also approximately parallel to the intrusive contact.

The most salient feature of the structure of the intrusion is the strong obliquity between the layering and the walls of the intrusion in the central segment. If we consider the entire intrusion (Fig. 3, stereographic nets), there is some dispersion in the measurements of the banding, but the best plane remains similar to the orientation in Lanjian pit, at ca. 095°E/50°N. This contradicts the previous

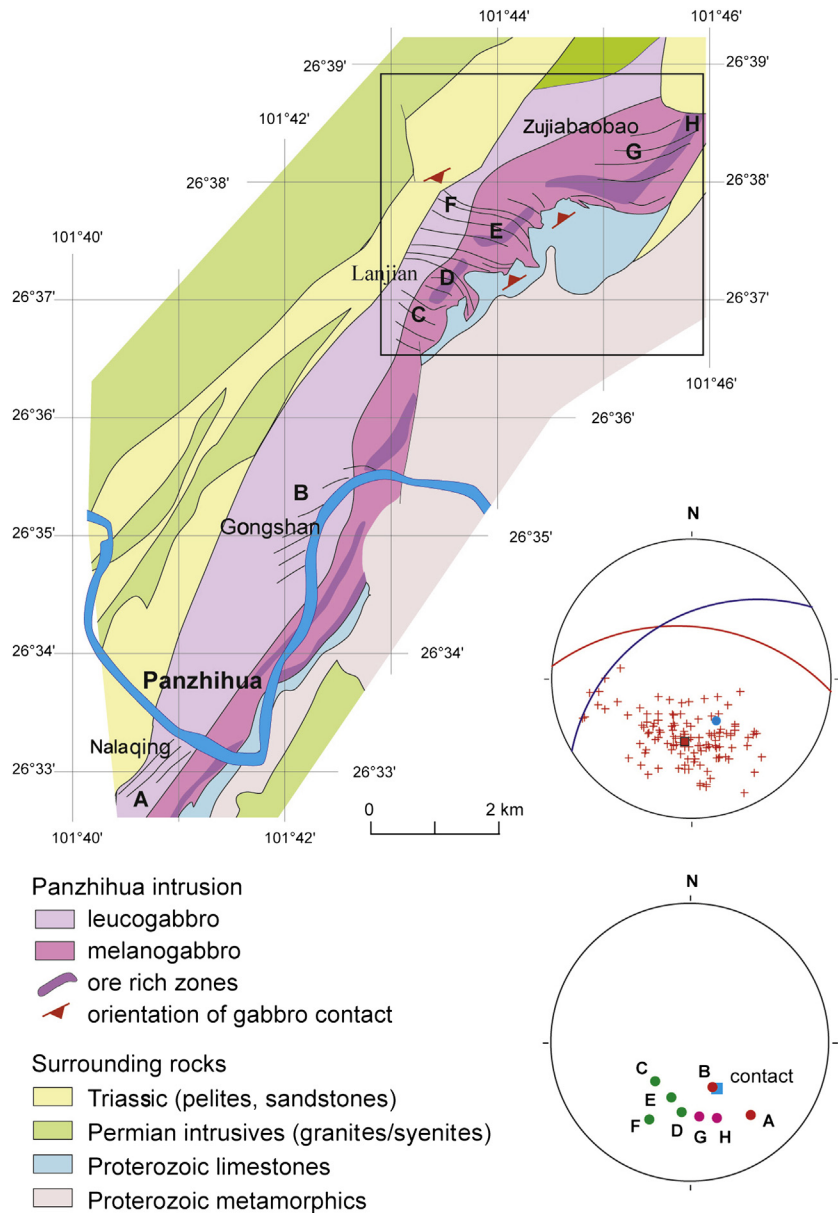


**Figure 3.** Map of the Panzhuhua intrusion (geology from Zhou et al., 2005, modified). Trace of the layering in the intrusion is interpolated from our measurements. Upper canvas: bulk set of layering orientations measured in the whole intrusion (calculated best plane:  $094^{\circ}\text{E}/50^{\circ}\text{N}$ , figured by its pole and its cyclographic trace) and orientation of the eastern contact in the Lanjian–Zujiabaobao open pits (average values:  $59^{\circ}\text{E}/43^{\circ}\text{NW}$ , pole and cyclographic trace). Lower canvas, average orientations (calculated best planes) of the layering in the intrusion for zones A–G. Wulff stereographic projection, lower hemisphere.

interpretation that the intrusion is a large sill whose floor was the present-day southeast contact of the intrusion. Were this the case, the layering should be parallel to the contact. Our observations show instead that the intrusion has a more complex form comprising a central discordant segment that separates two concordant segments. In the central dyke-like segment, the layering is oblique to the footwall, whereas in the southern and northern parts, the geometry is much closer to that of a sill. In section, the intrusion would have a flattened “stair case” shape.

### 3.2. The discordant eastern contact of the intrusion in Lanjian area

In Lanjian open pit, the layering of the gabbro is highly oblique to the contact, which is well exposed and preserved in three large panels of dolomite (now metamorphosed to marble by contact

metamorphism). These panels allow us to establish a more precise 3D geometry of the contact (Fig. 6).

Numerous faults have been observed and measured in the Lanjian pit. Their orientation is variable, with no clearly predominant population (stereographic net, Fig. 6). Displacements along these faults are difficult to estimate accurately, due to lack of good markers. Most of the time, the offset seems to be low, probably less than few metres. The north-eastern contact in panel 2 is a thin reverse shear-zone (labelled F4, Fig. 6) that displays an S-C type fabric. It is parallel to the contact, and disrupts neither its bulk continuity nor its orientation in this area. It is soon lost eastwards, and the intrusive contact is preserved around point C. A few steep N–S and NW–SE faults can be followed for longer distances, and cut across the eastern contact. They separate the three panels (1–3, Fig. 6), as already mapped by Zhou et al. (2005). The fault F2, at the

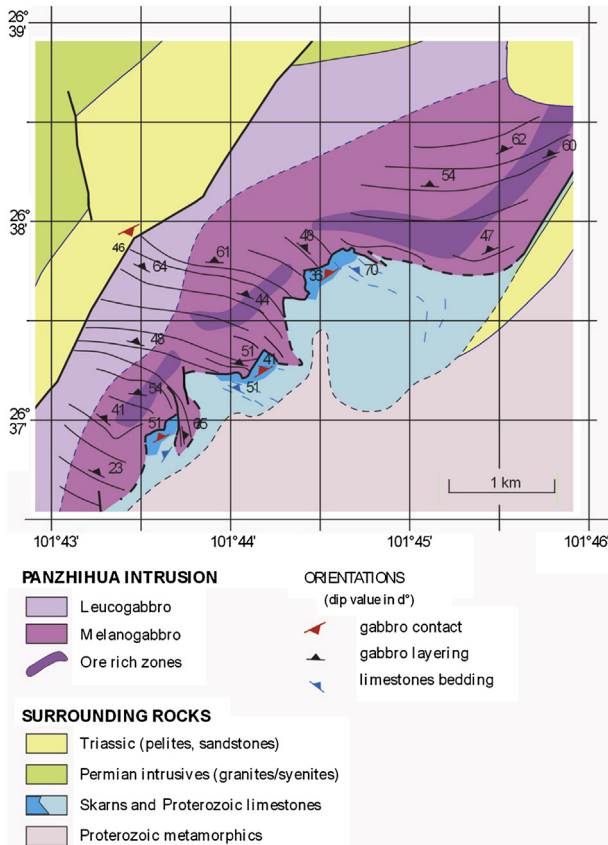


**Figure 4.** Map of the gabbro and surrounding rocks in the Lanjian–Zujiabaobao open pits (area delimited Fig. 3). The leucogabbro-melanogabbro limit, the distribution of ore bodies and the eastern contact of the limestone are schematic and adapted from previous work.

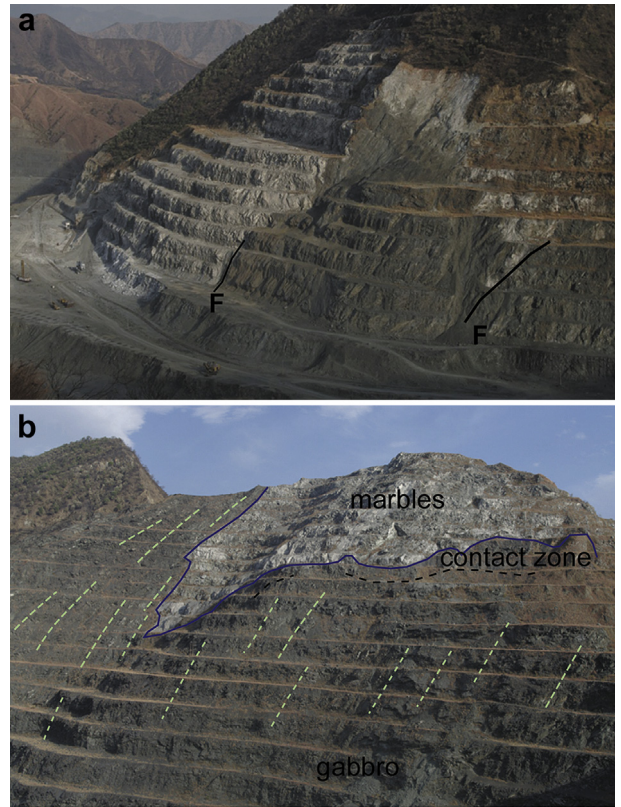


**Figure 5.** (a) The irregular contact between footwall marble (white to brown) and gabbro (grey) in the northern Lanjian open pit (see Fig. 6, label 3). Foliation in the gabbro is at  $\sim 30^\circ$  of the average contact surface. (b) Contact between marble and gabbro in the central Lanjian open pit (Fig. 6, area B). Foliation in the gabbro underlined by green dotted lines. It is at  $\sim 15^\circ$ – $\sim 40^\circ$  of the contact surface. Dotted black line: approximated limit of the contact zone, mainly made of fine grained amphibolites.

eastern contact of the southernmost marble panel (latitude N  $26^\circ 37'$ , Fig. 6) is a ductile fault, marked by pinched segments of marble with C-S lenses and mylonitic schistosity. Adjacent to the fault, the banding in the gabbro rotates to become parallel to the fault. Therefore this fault, which according to Zhou et al. (2005) does not displace the western faulted contact of the intrusion, could be an early fault that only affected the still-ductile gabbro.

To estimate offsets on the larger faults, as well as their influence on the structural orientation of the gabbro, we used the gabbro-marble contact as marker. This contact can be accurately drawn from map data, using field GPS positions. We complemented our field data with satellite images, because the contrast in colour between marble and gabbro makes the contact easy to follow. Once we had precisely fixed the position and altitude of the contact at enough pin points, it was possible to define its geometry (dip and orientation) in each panel by a series of horizontal contour lines through the pin points (Fig. 6). Such a basic construction remains imprecise, because it smoothes the intrusive contact, assuming it to be a plane at the scale of each panel. The actual contact is highly irregular at metric scale, or can be curved at the pit scale. For instance, the contact shown Fig. 5 (area N–E of fault F6, Fig. 6) is clearly not a plane, but has rather a concave spoon shape. Nevertheless, the construction clearly shows the following features:

- contacts in panels 2 and 3 (North Lanjian and central Lanjian) lie in or very near the same plane. The set of faults F5–F6, which have a clear morphological imprint in the upper part of the pit wall, have no significant offsets at the intrusion scale.

- contacts in panels 1 and 2 clearly lie in two different planes. From the construction, it can be inferred that faults F2 and F3 have a sinistral strike-slip movement, as indicated on the Zhou et al. (2005) map. We estimate that the horizontal sinistral component of the offset could have been more than 400 m. But the orientation of the contact in panel 1 remains within  $10^\circ$  of its orientation in panels 2 and 3; in other words, the faulting does not influence the orientation of the contact. This continuity in orientation of the contact from panel 1 to panel 3 indicates that the set of N–S faults did not significantly rotate the marbles, nor the gabbros, from one block to another.

We also used the Gocad modeller to better visualize the shape of the gabbro-marble contact (Fig. 7). In each case, the 3 panels have similar orientations of  $063^\circ/51^\circ$ NW,  $N55^\circ/36^\circ$ NW, and  $058^\circ/41^\circ$ NW (from SW to NE, i.e. panel 1–3), with a minor displacement between panels 2 and 3, and a larger one between panels 1 and 2. North of panel 3 (the area labelled 4, Fig. 6), between Lanjian and Zujiabaobao pits, a large offset of the contact corresponds to an apparent dextral displacement in an EW direction. We were unable to clearly identify any EW faults, i.e. possible dextral conjugate faults to NS sinistral faults, that could explain this geometry. Instead we believe that the contact is solely intrusive, and oriented in this area parallel to the layering of the gabbro (Fig. 4). In other words, in our interpretation, the initial igneous contact was highly irregular and its orientation changed from parallel to the layering in the northern and southern segments to highly oblique in the central segment.

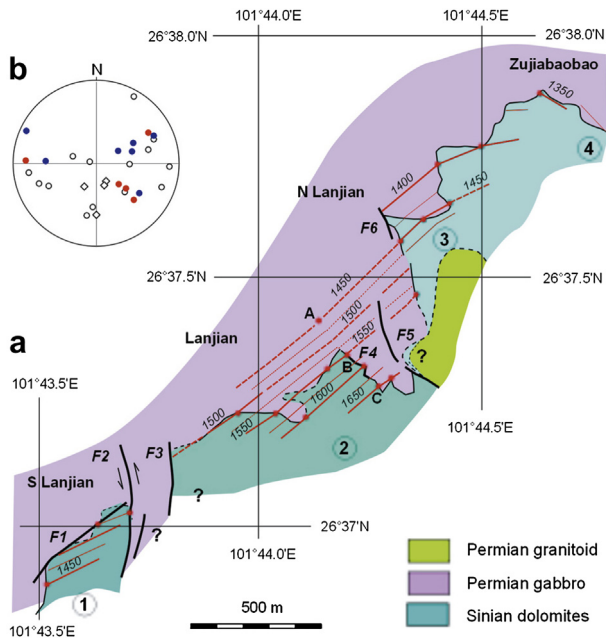


**Figure 6.** (a) Geometry of the eastern contact of the gabbro in the Lanjian pit. Field data, complemented by information from Google Earth images (date of the image: 2010/09/21). Plain lines: geological contacts, as directly mapped in the field, or non-ambiguous contacts from satellite images or field photographs. Dotted lines: extrapolated contacts, or contacts poorly known due to lack of outcrops. The trace of the gabbro-marble contact has been observed or estimated at 35 points, either from GPS measurements in the field, or from Google Earth 3D images (discrepancy between altitude from GPS and from Google Earth image are mostly in the range  $\pm 2$  m, but sometimes much more when the topography of the pit changed due to caving). Point A, Lanjian area, is a virtual contact point located as the extension of the B–C contact (the actual contact is at depth under the gabbro). Contact points have been used to define, or pin, the horizontal level curves of the gabbro-marble contact surface; the red dots represent a selection of pin points. Plain lines: level curves of good reliability. Dotted lines: extrapolated curves, or curves drawn through poorly defined pin points. (b) Stereographic net: 30 fault measurements from the Lanjian pit (blue dots: reverse faults; red dots: dextral strike-slip faults; black open circle: faults with undetermined movement; black open diamonds: along-bedding slip in the dolomites). Wulff stereographic projection, lower hemisphere.

Assuming that the layering of gabbro was initially close to horizontal, as discussed below, its orientation can be used to establish the original, pre-deformation, form of the intrusion. In the central segment (Lanjian area), we estimate that the initial orientation of the SE contact of the intrusion is  $N173^\circ E$ , dipping  $38^\circ W$ .

Away from the zone of contact metamorphism, the initial orientation of the sedimentary series is easily recognizable – the initial stratification of the limestone is readily identified by the presence of cherty shale beds that mark S0. Although the beds are moderately folded, the stratification is generally parallel to the layering of the gabbro.

### 3.3. The border zone

A separate contact facies is present in the gabbro along the margins of the intrusion: a 1–2 m wide chilled border, now altered to fine-grained amphibolite, gives way inward to coarser grained pegmatoid gabbro. Magnetite pods and layers, the ore bodies, are dispersed in the gabbro and underlying marble. Along discordant contacts, the magma of the main intrusion has invaded the wall rocks along bedding planes, separating wedges of marble that penetrate into the intrusion.

### 3.4. Dykes in the contact aureole

Multiple generations of mafic dykes intrude the marble of the metamorphic aureole (Fig. 8). Within the aureole, the marble is extremely deformed, as manifested by intense boudinage of early dykes, the formation of isoclinal folds with poorly aligned hinges, and the development of a metamorphic foliation that generally is parallel to the contact. The foliation in the marble, the abundance and orientation of boudins of mafic rock, and the complex, tight folding reflects considerable flattening at the wall of the intrusion.

The abundance of dominantly mafic dykes in the contact aureole reaches 20–30% in places. In the lower portion of the large dyke illustrated in Fig. 8a and b, the contacts are sharp and well preserved, but higher up the same dyke is strongly deformed (Fig. 8a). Several episodes of dyke emplacement are evident – a younger, relatively unaltered, dark-coloured portion has intruded between two older, more altered dykes. The original magmatic assemblage of the dyke has been replaced by an assemblage typical

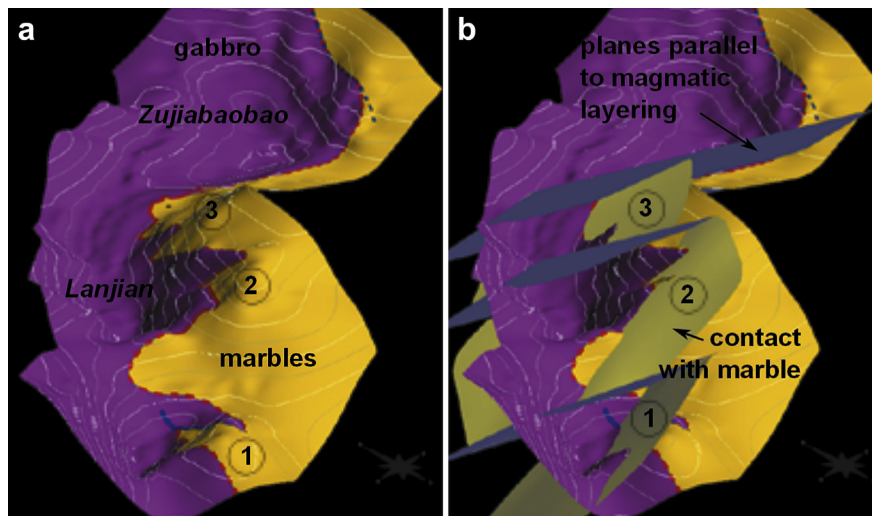


**Figure 7.** 3D Gocad images of the Lanjian and Zujiabaobao open pits. (a) The gabbro-limestone contact. 1 to 3: The 3 panels labelled 1 to 3, Fig. 6. (b) Modelled position of the contact planes of the 3 panels of marble. In grey, planes parallel to layering in the gabbro. The plane between panels 1 and 2 is not accurate because the north-south faults F5 and F6 (Fig. 6) are not taken into account. Notice the small offset between panels 2 and 3; the large offset north of panel 3 (zone 4, Fig. 6) can be explained by a contact parallel to the layering of gabbro (i.e. analogous to a contact at the base of a sill).

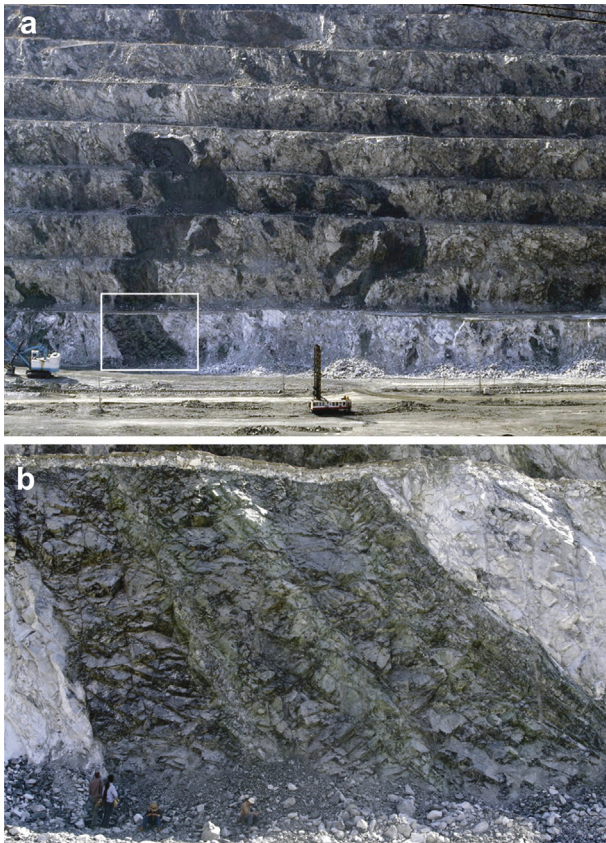


**Figure 8.** (a) General view of dykes at various stages of deformation and reaction with the contact aureole; (b) closer full of large dyke (identified by the white rectangle in (a)). A younger dyke intrudes in the centre between two other dykes. Note people on bottom left for scale.

of high temperature/low pressure metamorphism of mafic rock. In the central dyke large porphyroblasts of olivine and clinopyroxene lie in a matrix of brown hornblende, tremolite and chlorite. The compositions of dykes vary considerably: some have more evolved compositions manifested by an absence of olivine and the presence of abundant potassium feldspar; others have picritic compositions.

Many dykes show evidence of extensive interaction with surrounding marble, accompanied by progressive deformation. As a result of this interaction, the margins of the dykes have become undulated and diffuse, leading eventually to wholesale boudinage that transforms the dyke into a series of isolated pods. Centimetre-scale concentric bands defined by varying concentrations of silicate minerals commonly surround the dykes. In some cases, bands of forsterite, now serpentized and almost black, with or without spinel and diopside, alternate with bands of calcite, to produce what is known as “zebra rock” (Fig. 9a). In other cases the mineralogy is more complex as broader bands are variably rich in diopside, andradite and grossular garnet, calcic and potassic feldspar, and other calc-silicate minerals. In the companion paper (Ganino et al., 2013b) it is shown that this variation in mineralogy is largely due to differences in the composition of the protolith, particularly the proportion of silica minerals and clay. Deformation of bands rich in calc-silicate minerals produces complex folds, as illustrated in Fig. 9b.

An observation of considerable importance to our interpretation of the origin of the dykes and their relationship to the main intrusion is the lack of mafic dykes in outcrops remote from the intrusion. Although we did not undertake a systematic survey, we noted that dykes were totally absent in two small quarries in

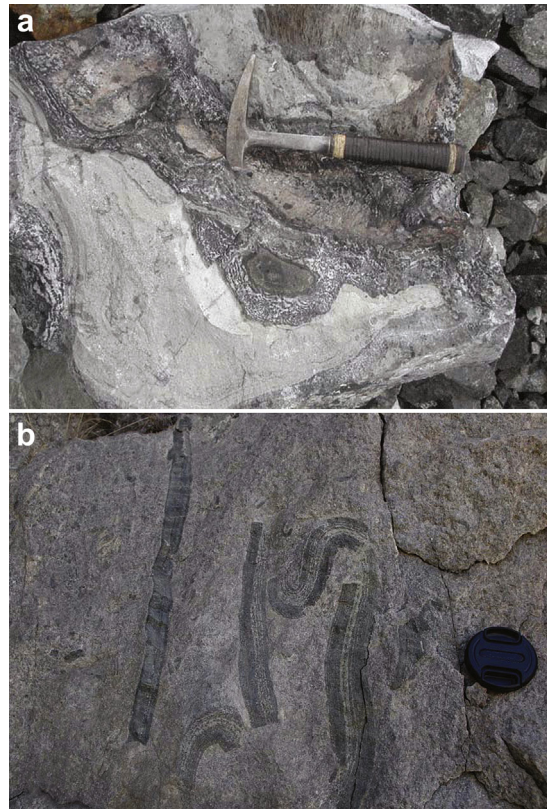


**Figure 9.** (a) Zebra rock. Alternating concentric bands of dark coloured serpentized olivine and white calcite surround blocks of highly altered chlorite. (b) Folded bands of calc-silicate rocks in melted dolomites.

dolostone to the east of the intrusion and in several outcrops to the northeast and northwest.

#### 4. A new model for the intrusion and its ore deposits

##### 4.1. Constraints

In previous papers, the Panzihua intrusion had been interpreted as a layered, differentiated sill and the ore deposits were thought to have formed at or near its floor. Our structural data require re-evaluation of these ideas. Critical to the interpretation are:

- (a) *The high angle between the layering in the intrusion and its contacts.* From our new observations and available maps, the general SSW–NNE contact can be separated in 3 segments: a southern segment and a northeastern segment, where the gabbro banding is roughly parallel to the contact and orientated approximately SW–NE; and a central segment, striking N–S, where the banding is more oblique to the contact. We were not able to map the NW, presumably upper, contact of the intrusion, which was faulted wherever we saw it: Chinese maps locate the fault about 400 m from the SE contact.

If the layering is magmatic, as seems logical given the similarity between this structure and layering in numerous other intrusions (e.g. Cawthorn, 1996), then its original orientation probably was not far from horizontal. Although original inclinations of up to 45° are reported in some intrusions (e.g. Wager and Deer, 1939; Ferguson and Pulvertaft, 1963), in most intrusions, initial dips are less than 20°. If this angle is assumed

for the central segment, the SE contact that we mapped in detail was initially moderately inclined, with a dip between 20 and 40° (Figs. 6 and 10)

- (b) In the central segment, the magmatic layering, rather than being parallel to the near-horizontal base of a sheet-like sill, is highly oblique to the steeply dipping contact. The layering persists from one end of the intrusion to the other and if this layering was subhorizontal, the southern end was originally about 3–4 km deeper than the northern end.
- (c) In the central segment, the contact between melanogabbro and leucogabbro is not parallel to the horizontal floor of the intrusion but, from the pattern shown in the published map (Zhou et al., 2005; Pang et al., 2008), is aligned parallel to the sloping wall of the intrusion.
- (d) In the central segment, the ore deposits are distributed along the steeply dipping wall of the intrusion and not along its floor. Rather than being a discontinuous, near-horizontal sheet of ore, as in the previous interpretation, the deposits occur as individual pods at different heights along the contact. The main deposit in the Zujibaobao open pit in the NE, for example, was originally located 800 m above the deposit in the Lanjian open pit in the SW (see Figs. 3 and 4).
- (e) The scalloped, irregular nature of the contact suggests that magma of the main intrusion actively invaded its country rocks.
- (f) The abundance of mafic dykes within the contact aureole and their differing states of deformation and extent of interaction with the marble is evidence that mafic magmas were injected, for a protracted period, into the rocks surrounding the intrusion. The diversity of chemical compositions of the dykes (reported by Ganino et al., 2013a) indicates that the dykes were not co-magmatic with the main intrusion and came from another source.
- (g) The mafic magma interacted with the carbonate, forming calc-silicate rocks and releasing abundant CO<sub>2</sub> (Ganino et al., 2008). Given the slope of the contact, which places the intrusion above the aureole, at least part of this chemical flux must have passed upwards and through the Panzhihua intrusion itself.

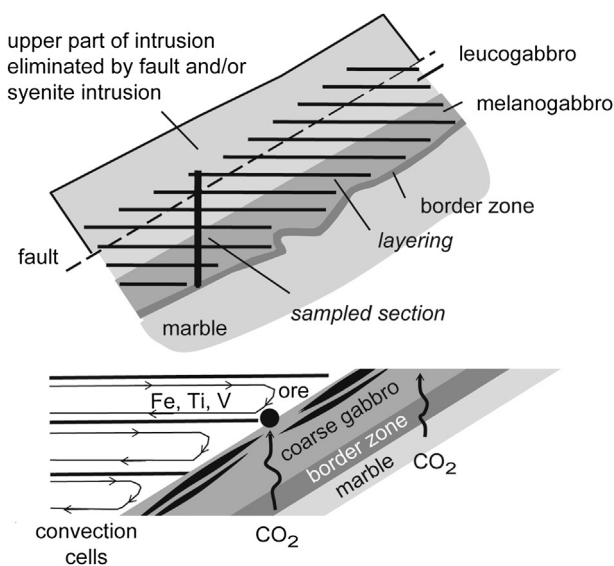


**Figure 10.** Schematic representation of part of the SE contact of the central segment showing relationship between layering, the border zone and the contact with marble. Also shown is the transition from melanogabbro to leucogabbro and suggestion of where Pang et al. (2008) sampling was made, so as to remain perpendicular to the layering while passing from one lithology to the other.

## 4.2. Magmatic aspects

### 4.2.1. Shape and orientation of the intrusion

Key to our interpretation of the form in the intrusion is the layering. In the view of Zhou et al. (2005) and Pang et al. (2008), and from our own observations, this layering strongly resembles that in other large, differentiated mafic-ultramafic intrusions such as the Bushveld, Skaergaard or Muskox (Cawthorn, 1996). In these intrusions, the orientation of the layering is close to horizontal, except in border zones. In the Panzhihua intrusion, a border zone is indeed present – it comprises the thin, fine-grained layer that recrystallized as amphibole-rich gabbro and the isotropic pegmatoid gabbro – but inward from this zone most parts of the intrusion are layered. The border zone can be traced along most of the contact: where the layering is parallel to the contact, as in the northern and southern segments, the border zone is concordant and parallel to the layering; where the contact with country rock is oblique, as in the central segment, the border zone is discordant (Figs. 4, 5, 10 and 11).

Our preferred interpretation is that, as in the other intrusions, the layering originally was horizontal. If so, only the northern and southern segments of the Panzhihua intrusion had a sill-like form: in the central segment, the contact had a moderate dip. If we use the layering to define the original horizontal direction, we can eliminate the effects of later tilting and deformation. This results in the shape shown in Fig. 11, a section showing that the intrusion as a large, moderately dipping dyke that links two sill-like portions. In this interpretation, the southern segment was originally 3–4 km deeper than the northern segment, and the contact between melanogabbro and leucogabbro was not horizontal but dipped at a moderate angle in the central segment.

We recognize that magmatic layering is not always horizontal and that many examples of steeply inclined layering have been recorded (Upton et al., 1996). In most such cases, however, such layering is oriented parallel to the margins of the intrusion; e.g. the concentric layering in Alaskan-type intrusions (Irvine, 1974). In the northern and southern segments of the Panzhihua intrusion, i.e. in the segments where we assume a sill-like geometry, the layering is indeed parallel to the contact, but this is not the case in the enigmatic central segment. We are impressed by the overall similarity of the form, the scale and the mineralogical expression of the layering in segments where it is parallel and where it is oblique to the contacts, and use this similarity to argue for a similar origin in both cases. If this view is accepted, then the most reasonable interpretation is that the layering was originally horizontal.

The dyke-like form shown in Fig. 11 is based on the assumption that the intrusion was not very much broader than the ~1 km shown in published maps: i.e. that the fault that bounds the northwestern margin has not removed a major portion of the intrusion. We envisage the intrusion as an S-shaped, sheet-like,

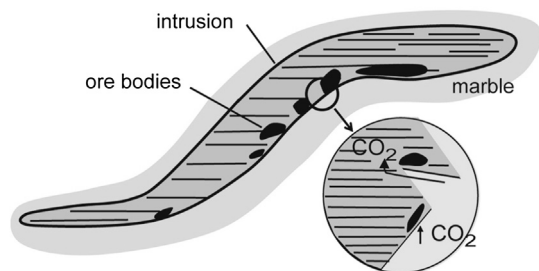


**Figure 11.** Sketch of a section through the Panzhihua, with a detailed view of part of the contact. Fluids rich in CO<sub>2</sub> released by decarbonatization of wall-rock dolomites flowed into the intrusion, triggering the formation of ore deposits.



concentrically zoned body, with leucogabbro at the centre and melanogabbro at both margins, the northwestern part having been removed by the fault (Fig. 3). We cannot exclude, however, the possibility that the intrusion was originally far broader, and that the contact we mapped was one side of a large lopolith or funnel-shaped intrusion.

#### 4.2.2. Emplacement and solidification of the intrusion

In this section we discuss how the intrusion was emplaced and how it solidified. In particular we need to explain, in the light of our new interpretation of the structure of the intrusion, the origin of both the layering, and the mafic to more felsic differentiation of the intrusion.

In previous interpretations, this layering was interpreted to have formed in a conventional manner as crystals of olivine, pyroxene, magnetite and plagioclase accumulated on the floor of the sill-like intrusion, either through in-situ growth or gravitative settling. In this model, solidification would have advanced upwards from the floor of the intrusion, and the extraction of early-forming crystals would have led to an evolution in the composition of the residual liquid, from melanogabbro at the base through to leucogabbro at the top. This interpretation is untenable, however, in a relatively narrow, steeply inclined dyke (Fig. 11). In such an intrusion, heat loss to surrounding wall rocks would have been greater than heat loss through the roof, and the magma would have solidified inwards from both contacts, not upwards from the base. The layering cannot therefore be interpreted as having formed on the floor of the intrusion and it must have another origin.

McBirney and Noyes (1979), Irvine (1980) and Huppert and Sparks (1984) have described how a hot fluid may develop a particular type of convection characterized by the presence of a series of horizontal layers, each of which convects independently. The name “double-diffusive convection” is used to describe the system because both heat and matter diffuse across the boundaries between the cells. What results is a gradient in both temperature and composition of the liquid, from mafic and hot at the base to more evolved and cooler near the top. If solidification proceeds inwards from the walls of such a body, the convecting cells freeze into place, producing a layered structure. As discussed below, this model provides an explanation for both the layering and the differentiation of the Panzhihua intrusion.

We imagine that the body solidified inward and that the broad-scale layering was inherited directly from the convecting cells. Finer-scale layering may have resulted from current deposition or oscillations in the conditions of crystallization. Dominantly mafic minerals accumulated in the early-solidifying margins, concentrating more evolved magma in the centre of the intrusion. The magma body thereby differentiated parallel to its steeply dipping contacts, from mafic at the margins to more evolved at the centre (Figs. 10 and 11). The sections displaying a change in composition from melanogabbro to leucogabbro were sampled by Pang et al. (2008) in a direction near-perpendicular to the layering. They had assumed that these sections had passed from the base to top of a sill-like body; instead they may have passed obliquely from the margin to the centre of a laterally differentiated dyke, as shown in Fig. 10.

In the absence of a complete structural map of the intrusion and its surroundings, we have few direct constraints on mechanism of intrusion. We do not know, for example, if room for the intrusion was made by expansion of a fracture along which the magma penetrated, or by replacement of the wall rocks. However, given the significant width of the intrusion, the irregular geometry of the contact and the evidence of partial melting of marble (Ganino et al., 2013a), the latter process was certainly involved. The implication is that large volumes of carbonate host rock were assimilated into the intrusion or lost into the environment.

For most of its exposed length, the Panzhihua intrusion is an irregularly shaped discordant dyke; concordant sill-like sections are limited to the two ends. To the southwest the intrusion appears to pinch out, but to the northeast it disappears under younger sedimentary rocks. It is likely that it extends farther in this direction. This raises the possibility that the steeply dipping part of the intrusion is the edge of a large saucer-shaped intrusion of the type described by Chevallier and Woodford (1999) and Svensen et al. (2006) in sedimentary basins in South Africa and off the coast of Norway. Further geological and structural mapping is needed before it can be established whether the Panzhihua intrusion, as well as other nearby intrusions (Hongge, Baima), have this geometry. Given the restriction of large mafic-ultramafic intrusions and Fe-Ti-V ore deposits to a narrow corridor extending north from Panzhihua, it is possible that all the intrusions form part of a single magma system.

#### 4.2.3. Notion of a magma corridor

To explain the abundance of mafic dykes in the metamorphic aureole, the diversity of compositions of these dykes (Ganino et al., 2013a), and the absence of dykes in the country rock away from the intrusion, we propose the following model (Fig. 12). We imagine that a zone of weakness in the crust – a large fault or shear zone or a zone of enhanced magma permeability – guided the emplacement of the first dykes. These intrusions heated the wall rocks, reducing their strength and facilitating emplacement of subsequent dykes. The Panzhihua intrusion then invaded the magma corridor, accompanied by the intrusion of additional dykes. The intrusion of several hundred metres of dense, Fe-rich magma, and transfer of heat into the wall rocks, caused the deformation of both the sedimentary rocks and earlier-intruded dykes.

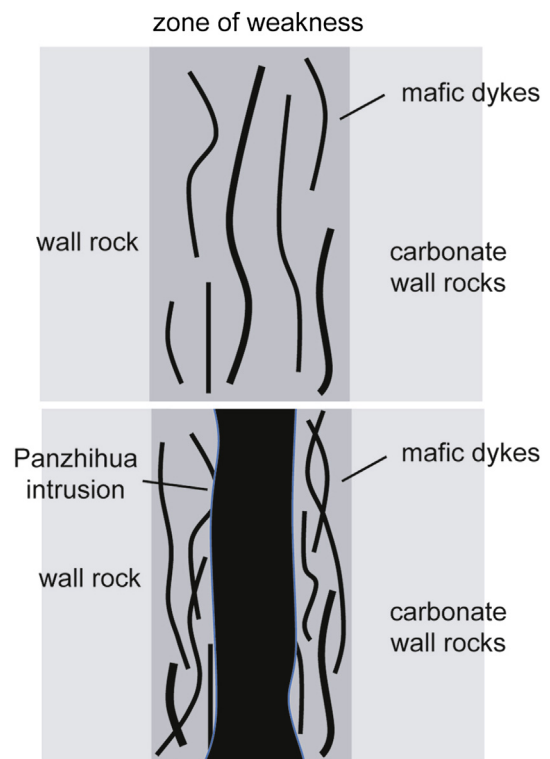


**Figure 12.** Sketch illustrating the notion of a magma corridor. Dykes initially intrude along a zone of weakness in the crust and guide the subsequent intrusion of the Panzhihua body.

#### 4.3. Formation of the ore deposits

The Panzhihua ore bodies, like many other magmatic ore deposits, contain a disproportionate quantity of ore metal. The chemical analyses and petrological descriptions of Zhou et al. (2005) show that the ore bodies contain an average of about 25 wt.% Fe<sub>2</sub>O<sub>3</sub>, 6.2 wt.% TiO<sub>2</sub> and 1375 ppm V. If the parental magma had a composition like that of the picrites of the Emeishan flood volcanic series – i.e. between 11 and 16 wt.% Fe<sub>2</sub>O<sub>3</sub>, 2.4 and 3.9 wt.% TiO<sub>2</sub> and 295 and 438 ppm V (Xu et al., 2001), this implies enrichment factors of 2–4. If the magma crystallized in a closed system, it is difficult to account for the large quantity of Fe and Ti contained within the ores. In the case of deposits within a sill or conduit, the ore mineral can be assumed to segregate from magma flowing through the system, in which case the source was a much larger amount of magma than is present in the intrusion itself. If the Panzhihua magma chamber were divided into a series of independently convecting cells, the presence of these cells would preclude sustained flow of magma through the conduit.

In this context we refer to the conclusions reached by Ganino et al. (2008, 2013a) who used the texture and compositions of marbles adjacent to the contact to infer that these rocks underwent decarbonatization and partial melting. The carbonate partial melts, and the fluids released by decarbonatization, are less dense than the solid rocks and they would have migrated upwards, eventually to reach the sloping contact of the intrusion. Part of the fluids might migrate laterally along the contact, but in places where the carbonate is deeply indented into the intrusion of where the contact is sloping, the fluids will stream upwards from the protrusion and into the magma (Figs. 10b and 11).

The upward migration of complex CO<sub>2</sub>-H<sub>2</sub>O fluids or melts through the Panzhihua intrusion had several important effects. At the moderate pressures corresponding to the shallow level at which the intrusion was emplaced, the solubility of CO<sub>2</sub> in silicate liquid is very low. In addition, when silicate liquid interacts with a CO<sub>2</sub>-H<sub>2</sub>O fluid, water partitions strongly into the fluid. When the CO<sub>2</sub>-H<sub>2</sub>O fluid migrated upwards through Panzhihua intrusion, it dehydrated the magma, causing it to become supersaturated in silicate phases and triggering crystallization (Ganino et al., 2008). This process will complement the cooling resulting from the injection of relatively cool fluid into the magma. At the same time, the fluid oxidized the magma, promoting the crystallization of magnetite – the ore mineral. Convection in each cell would have transported Fe, Ti and V from the interior of the intrusion to the margins where crystallization and accumulation of oxides occurred (Fig. 10b). These minerals accumulated at sites along the sloping wall of the intrusion where protuberances or faults focussed a stream of fluid up into the overlying magma to form the ore bodies (Figs. 10 and 11).

Our studies at Panzhihua reveal several interesting aspects of the dyke-like segments of the intrusion. In addition to their possible role in the development of the Fe-Ti ore deposits, the form of the intrusion, the presence of abundant mafic dykes in the aureole, and the complex geometry of the contact must be taken into account when calculating the quantity of CO<sub>2</sub> and other greenhouse gases released to the environment. Ganino et al. (2008) and Ganino and Arndt (2009) calculated that a total of up to 74 Gt of CO<sub>2</sub> were released during emplacement of the Panzhihua intrusion. In their calculation they assumed that the aureole was about 300 m thick, a figure that is far greater than can readily be accounted for by conduction of heat from the main Panzhihua intrusion. It is probably that the excessive width of the Panzhihua aureole is due in part to heat supplied by the numerous mafic dykes in the aureole and circulation of fluids driven by the main intrusion and these dykes. Ganino et al.'s calculation did not take into account: (1) the CO<sub>2</sub>

released during the decarbonatization zones that surround the mafic dykes within the aureole, and (2) the probability of massive assimilation of carbonate wall rocks during emplacement of the discordant portions of the intrusion. Quantification of these contributions, which we expect to be on the same order as those already estimated by Ganino et al. (2008) and Ganino and Arndt (2009) must await more detailed structural mapping and petrographic-geochemical studies of the intrusion and its contact aureole.

#### 5. Conclusions

Our new mapping has revealed that the Panzhihua intrusion is an irregularly shaped discordant dyke with concordant, sill-like sections at both ends. Fractional crystallization inward from its margins produced a change in lithology from melanogabbro to leucogabbro. Magmatic layering in the intrusion may have been inherited from the development of multiple convection cells. Several types of mafic magma intruded as dykes into carbonate wall rocks, creating a thick, heterogeneous metamorphic aureole. CO<sub>2</sub>-rich fluids liberated by decarbonatization of these rocks oxidized the magma of the main intrusion, promoting the crystallization of Fe-Ti-V oxides and leading to the formation of the ore deposits.

#### Acknowledgements

The study is partially supported by a Famous overseas professor project MS2011ZGDZ[B]019 through China University of Geosciences (Beijing) and by the USA NSF "Continental Geodynamics" program. Geologists from the Panzhihua mining company are thanked for their logistic support. We gratefully acknowledge the considerable help in the field and warm support of our project provided by Mei-fu Zhou, Danping Yan and students. The manuscript benefited from constructive comments by 2 reviewers and editorial guidance by Professor M. Santosh.

#### References

- Cawthorn, R.G., 1996. Layered Intrusions. Elsevier, Amsterdam, 531 pp.
- Chevallier, L., Woodford, A., 1999. Morpho-tectonics and mechanism of emplacement of the dolerite rings and sills of the western Karoo, South Africa. *South African Journal of Geology* 102, 43–54.
- Ferguson, J., Pulvertaft, T.C.R., 1963. Contrasted styles of igneous layering in the Gardar province of South Greenland. *Mineralogical Society of America Special Paper* 1, 10–21.
- Ganino, C., Arndt, N.T., Zhou, M.-F., Gaillard, F., Chauvel, C., 2008. Interaction of magma with sedimentary wall rock and magnetite ore genesis in the Panzhihua mafic intrusion, SW China. *Mineralium Deposita* 43, 677–694.
- Ganino, C.L., Arndt, N.T., 2009. Climate changes caused by degassing of sediments during the emplacement of large igneous provinces. *Geology* 37, 323–326.
- Ganino, C., Arndt, N.T., Chauvel, C., Alexandre, J., Athurion, C., 2013a. Melting of carbonate wall rocks and formation of the heterogeneous aureole of the Panzhihua intrusion, China. *Geoscience Frontiers* 4, 535–546.
- Ganino, C., Harris, C., Arndt, N.T., Prevec, S.A., Howarth, G.H., 2013b. Assimilation of carbonate country rock by the parent magma of the Panzhihua Fe-Ti-V deposit (SW China): evidence from stable isotopes. *Geoscience Frontiers* 4, 547–554.
- Huppert, H.E., Sparks, R.S.J., 1984. Double-diffusive convection due to crystallization in magmas. *Annual Review of Earth and Planetary Sciences* 12, 11–37.
- Irvine, T.N., 1974. Petrology of the Duke Island Ultramafic Complex, Southeastern Alaska. *Memoir, The Geological Society of America*, Boulder, 240 pp.
- Irvine, T.N., 1980. Magmatic infiltration metasomatism, double-diffusive fractional crystallization, and adcumulus growth in the Muskox intrusion and other layered intrusions. In: Hargraves, R.B. (Ed.), *Physics of Magmatic Processes*, Princeton University Press, Princeton, pp. 325–384.
- McBirney, A.R., Noyes, R.M., 1979. Crystallization and layering of the Skaergaard Intrusion. *Journal of Petrology* 20, 487–564.
- Pang, K.N., Zhou, M.F., Lindsley, D.H., Zhao, D., Malpas, J., 2008. Origin of Fe-Ti oxide ores in mafic intrusions: evidence from the Panzhihua intrusion. *Journal of Petrology* 49, 295–313.
- Shellnutt, J.G., Wang, K.-L., Zellmer, G.F., Iizuka, Y., Jahn, B.-M., Pang, K.-N., Qi, L., Zhou, M.-F., 2011. Three Fe-Ti oxide ore-bearing gabbro-granitoid complexes in

- the Panxi region of the Emeishan large igneous province, SW China. *American Journal of Science* 311, 773–812. <http://dx.doi.org/10.2475/09.2011.02>.
- Svensen, H., Jamtveit, B., Planke, S., Chevallier, L., 2006. Structure and evolution of hydrothermal vent complexes in the Karoo Basin, South Africa. *Journal of the Geological Society, London* 163, 671–682.
- Upton, B.G.J., Parsons, I., Emeleus, C.H., Hodson, M.E., 1996. Layered alkaline igneous rocks of the Gardar Province, South Greenland. *Developments in Petrology* 15, 331–363.
- Wager, L.R., Deer, W.A., 1939. Geological investigations in east Greenland, Part III. Petrology of the Skaergaard intrusion, Kangerdlugssuaq, east Greenland. *Meddelelser om Gronland* 105/4, 1–352.
- Wang, C.Y., Zhou, M.-F., 2006. Genesis of the Permian Baimazhai magmatic Ni–Cu–(PGE) sulfide deposit, Yunnan, SW China. *Mineralium Deposita* 41, 771–783. <http://dx.doi.org/10.1007/s00126-006-0094-2>.
- Xu, Y., Chung, S.L., Jahn, B.M., Wu, G., 2001. Petrologic and geochemical constraints on the petrogenesis of Permian-Triassic Emeishan flood basalts in southwestern China. *Lithos* 58, 145–168.
- Zhang, Z., Mao, J., Saunders, A.D., Ai, Y., Li, Y., Zhao, L., 2009. Petrogenetic modeling of three mafic–ultramafic layered intrusions in the Emeishan large igneous province, SW China, based on isotopic and bulk chemical constraints. *Lithos* 113, 369–392. <http://dx.doi.org/10.1016/j.lithos.2009.04.023>.
- Zhong, H., Zhou, X.H., Zhou, M.-F., Sun, M., Liu, B.G., 2002. Platinum-group element geochemistry of the Hongge Fe–V–Ti deposit in the Pan–Xi area, southwestern China. *Mineralium Deposita* 37, 226–239. <http://dx.doi.org/10.1007/s00126-001-0220-0>.
- Zhong, H., Yao, Y., Hu, S.F., Zhou, X.H., Liu, B.G., Sun, M., Zhou, M.-F., Viljoen, M.J., 2003. Trace-element and Sr–Nd isotopic geochemistry of the PGE-bearing Hongge layered intrusion, southwestern China. *International Geology Review* 45, 371–382. <http://dx.doi.org/10.2747/0020-6814.45.4.371>.
- Zhong, H., Yao, Y., Prevec, S.A., Wilson, A.H., Viljoen, M.J., Viljoen, R.P., Liu, B.-G., Luo, Y.-N., 2004. Trace-element and Sr–Nd isotopic geochemistry of the PGE-bearing Xinjie layered intrusion in SW China. *Chemical Geology* 203, 237–252. <http://dx.doi.org/10.1016/j.chemgeo.2003.10.008>.
- Zhong, H., Qi, L., Hu, R.-Z., Zhou, M.-F., Gou, T.-Z., Zhu, W.-G., Liu, B.-G., Chu, Z.-Y., 2011. Rhenium–osmium isotope and platinum-group elements in the Xinjie layered intrusion, SW China: implications for source mantle composition, mantle evolution, PGE fractionation and mineralization. *Geochimica et Cosmochimica Acta* 75, 1621–1641. <http://dx.doi.org/10.1016/j.gca.2011.01.009>.
- Zhou, M.F., Yang, Z.X., Song, X.Y., Keays, R.R., Leshner, C.M., 2002. Magmatic Ni–Cu–(PGE) sulfide deposits in China. In: Cabri, L.J. (Ed.), *The Geology, Geochemistry, Mineralogy, and Mineral Beneficiation of the Platinum-group Elements*, Special vol. 54. Canadian Institute of Mining, Metallurgy and Petroleum, pp. 619–636.
- Zhou, M.-F., Robinson, P.T., Leshner, C.M., Keays, R.R., Zhang, Cheng-Jiang, Malpas, J., 2005. Geochemistry, petrogenesis and metallogenesis of the Panzhihua Gabbroic layered intrusion and associated Fe–Ti–V oxide deposits, Sichuan Province, SW China. *Journal of Petrology* 46/11, 2253–2280.
- Zhou, M.F., Arndt, N.T., Malpas, J., Wang, C.Y., Kennedy, A.K., 2008. Two magma series and associated ore deposit types in the Permian Emeishan Large Igneous Province, SW China. *Lithos* 103, 352–368.